

7N-02  
197159  
198.

# TECHNICAL NOTE

## D-141

EFFECT OF LOCALIZED MASS TRANSFER NEAR THE STAGNATION  
REGION OF BLUNT BODIES IN HYPERSONIC FLIGHT

By Paul M. Chung

Ames Research Center  
Moffett Field, Calif.

NATIONAL AERONAUTICS AND SPACE ADMINISTRATION  
WASHINGTON

May 1960

(NASA-TN-D-141) EFFECT OF LOCALIZED MASS  
TRANSFER NEAR THE STAGNATION REGION OF BLUNT  
BODIES IN HYPERSONIC FLIGHT (NASA) 19 p

N89-70574

Unclas  
00/02 0197159

## NATIONAL AERONAUTICS AND SPACE ADMINISTRATION

---

TECHNICAL NOTE D-141

---

## EFFECT OF LOCALIZED MASS TRANSFER NEAR THE STAGNATION

## REGION OF BLUNT BODIES IN HYPERSONIC FLIGHT

By Paul M. Chung

## SUMMARY

The effect of localized mass transfer on skin friction and heat transfer is studied analytically for the impervious surfaces downstream of the transpiration-cooled region of hypersonic blunt bodies.

Coefficient of local skin friction and Stanton number are calculated near the stagnation regions of a circular cylinder and a sphere for the case of localized mass transfer at the stagnation region.

The numerical results obtained and an existing result for a flat plate are compared on the basis of the Blasius dimensionless fluid injection parameter. The comparison shows that the localized mass transfer becomes less effective in protecting the downstream impervious surfaces when a favorable pressure gradient is imposed on the flow and when the flow is varied from two- to three-dimensional.

## INTRODUCTION

Mass transfer cooling, whether it is by ablation or injection of fluid through a porous wall, is likely to be applied in a localized region. The effect of upstream transpiration on the downstream solid surface was studied for a flat plate in references 1 through 3.

According to the authors of references 1 and 2, similar analyses when applied to the stagnation region of blunt bodies have been unsuccessful. The major cause of this appears to be the effect of pressure gradient in the stagnation region. It was pointed out in reference 4 that the usual integral methods of solution of laminar boundary-layer equations fail in many instances when the effect of streamwise pressure gradient on the velocity profile becomes pronounced.

It was indicated in reference 5, however, that under hypersonic flight conditions, the direct effect of the pressure gradient on the velocity profile is very small when the surface of the vehicle is highly cooled. In the present paper, the hypersonic approximations given in

reference 5 will be used to study the effect of localized mass transfer at the stagnation region of blunt bodies. Direct application of the flat plate solutions of reference 2 will be made in the study.

# LIST OF SYMBOLS

$a_1$	coefficient of $\eta$ in polynomial velocity profile
$C$	$\left(\frac{\rho_w \mu_w}{\rho_e \mu_e}\right)^{0.2}$
$C_f$	coefficient of local skin friction for hypersonic boundary layer, $\frac{\tau_w}{(1/2)\rho_e u_e^2}$
$\bar{C}_f$	coefficient of local skin friction for flat plate given in reference 2
$C_o$	$\frac{\rho \mu}{\rho_{e,o} \mu_{e,o}}$
$c_p$	specific heat at constant pressure
$F_1$	momentum thickness defined by equation (20)
$F_2$	momentum thickness defined by equation (23)
$f(\eta_B)$	Blasius function defined by equation (29)
$f_w$	Blasius blowing rate defined by equation (32)
$H$	$\frac{h_t}{h_{t,e}}$
$H_c$	ratio of displacement to momentum thickness
$h$	enthalpy defined by equation (5b)
$h_t$	total enthalpy defined by equation (5a)
$h^o$	heat of formation at zero temperature
$k$	thermal conductivity
$M$	molecular weight of mixture
$m$	mass fraction
$Pr$	Prandtl number

p	pressure
$q_w$	heat transfer rate per unit area to the surface
R	universal gas constant
r	distance from axis to point on surface of axisymmetric body defined in figure 1
St	local Stanton number, $\frac{q_w}{\rho_e u_{e,t} h_{t,e}}$
s	independent variable defined by equation (6)
T	absolute temperature
t	independent variable defined by equation (6)
U	$\frac{\partial \psi}{\partial t}$
u	x component of velocity
V	$-\frac{\partial \psi}{\partial s}$
v	y component of velocity
x	distance along surface from stagnation point
y	distance normal to surface
$\beta$	velocity gradient along surface at stagnation point, $\left(\frac{du_e}{dx}\right)_0$
$\delta$	thickness of boundary layer
$\delta_t$	modified boundary-layer thickness defined by equation (19)
$\eta$	$\frac{t}{\delta_t}$
$\eta_B$	Blasius variable defined by equation (31)
$\theta$	subtended angle to x
$\mu$	dynamic viscosity
$\nu$	kinematic viscosity
$\rho$	density
$\tau$	shear stress
$\psi$	stream function defined by equations (8) and (9)

## Subscripts

c	cylinder
e	edge of boundary layer
i	ith species
o	stagnation point
p	flat plate
s	sphere
w	surface
$\delta_t$	point corresponding to $t = \delta_t$

## Superscripts

$\wedge$	end of the transpiration-cooled region
'	total differentiation with respect to $\eta_B$

## ANALYSIS

The study begins with the following set of equations for the laminar boundary layer over two-dimensional or axisymmetric bodies (see fig. 1). The hypersonic boundary layer is assumed to be in chemical equilibrium and the Lewis number is assumed to be unity. Then,

$$\frac{\partial \rho u r^\epsilon}{\partial x} + \frac{\partial \rho v r^\epsilon}{\partial y} = 0 \quad \text{continuity} \quad (1)$$

$$\rho u \frac{\partial u}{\partial x} + \rho v \frac{\partial u}{\partial y} = \frac{\partial}{\partial y} \left( \mu \frac{\partial u}{\partial y} \right) + \rho_e u_e \frac{du_e}{dx} \quad \text{momentum} \quad (2)$$

$$\rho u \frac{\partial h_t}{\partial x} + \rho v \frac{\partial h_t}{\partial y} = \frac{\partial}{\partial y} \left( \frac{\mu}{Pr} \frac{\partial h_t}{\partial y} \right) + \frac{\partial}{\partial y} \left[ \mu \left( 1 - \frac{1}{Pr} \right) \frac{\partial}{\partial y} \left( \frac{u^2}{2} \right) \right] \quad \text{energy} \quad (3)$$

$$p = \rho \frac{R}{M} T \quad \text{state} \quad (4)$$

where

$$\epsilon = 0 \quad \text{for two-dimensional bodies}$$

$$\epsilon = 1 \quad \text{for axisymmetric bodies}$$

The diffusion equation is not necessary here because of the assumption of chemical equilibrium.

The total enthalpy,  $h_t$ , includes the chemical energy and is given by

$$h_t = \sum_i h_i m_i + \frac{u^2}{2} \quad (5a)$$

where

$$h_i = \int_0^T c_{p,i} dT + h_i^0 \quad (5b)$$

The conservation equations can be transformed to more convenient forms by defining a new set of independent variables  $s$  and  $t$  as

$$\left. \begin{aligned} s &= \int_0^x C_0(x) u_e(x) r^{2\epsilon}(x) dx \\ t &= u_e r^\epsilon \int_0^y \frac{\rho}{\rho_{e,0}} dy \end{aligned} \right\} \quad (6)$$

The symbol  $C_0$  in equation (6) represents the ratio

$$\frac{\rho\mu}{\rho_{e,0}\mu_{e,0}} = \left( \frac{\rho_e\mu_e}{\rho_{e,0}\mu_{e,0}} \right) \left( \frac{\rho\mu}{\rho_e\mu_e} \right)$$

and is a function of both  $x$  and  $y$ . A study of references 6 and 7 shows that for a Lewis number of 1 an approximate solution to the conservation equations can be obtained to predict the heat transfer within 10 percent of the exact solution. This is done by considering  $\rho\mu/\rho_e\mu_e$  to be independent of  $y$  and to be equal to

$$C = \left( \frac{\rho_w\mu_w}{\rho_e\mu_e} \right)_0^{0.2}$$

With this approximation:

$$C_0(x) = \left( \frac{\rho_e \mu_e}{\rho_{e,0} \mu_{e,0}} \right) C \quad (7)$$

Now, a stream function is defined by

$$\rho u r^E = \rho_{e,0} \frac{\partial \psi}{\partial y} \quad (8)$$

and

$$\rho v r^E = -\rho_{e,0} \frac{\partial \psi}{\partial x} \quad (9)$$

which satisfy the continuity equation. Then the momentum equation is transformed on the  $s$ - $t$  plane as

$$\frac{\partial \psi}{\partial t} \frac{\partial^2 \psi}{\partial t \partial s} - \frac{\partial \psi}{\partial s} \frac{\partial^2 \psi}{\partial t^2} = \nu_{e,0} \frac{\partial^3 \psi}{\partial t^3} + \frac{1}{u_e} \frac{du_e}{ds} \left[ \frac{\rho_e}{\rho} - \left( \frac{\partial \psi}{\partial t} \right)^2 \right] \quad (10)$$

If we define

$$U = \frac{\partial \psi}{\partial t}, \quad V = - \frac{\partial \psi}{\partial s}$$

then from equation (8)  $U = u/u_e$  and equation (10) becomes

$$U \frac{\partial U}{\partial s} + V \frac{\partial U}{\partial t} = \nu_{e,0} \frac{\partial^2 U}{\partial t^2} + \frac{1}{u_e} \frac{du_e}{ds} \left[ \frac{\rho_e}{\rho} - \left( \frac{u}{u_e} \right)^2 \right] \quad (11)$$

The last term of the above equation appeared in essentially this form in the affinely transformed momentum equation in reference 5 where it was shown that the effect of this term on the solution of the complete equation is very small for highly cooled hypersonic boundary layers. Accordingly equation (11) is simplified to

$$U \frac{\partial U}{\partial s} + V \frac{\partial U}{\partial t} = \nu_{e,0} \frac{\partial^2 U}{\partial t^2} \quad (12)$$

The continuity equation becomes

$$\frac{\partial U}{\partial s} + \frac{\partial V}{\partial t} = 0 \quad (13)$$

The energy equation (3) is similarly transformed to

$$U \frac{\partial H}{\partial s} + V \frac{\partial H}{\partial t} = \frac{\nu_{e,o}}{\text{Pr}} \frac{\partial^2 H}{\partial t^2} + \nu_{e,o} \frac{u_{e,o}^2}{h_{t,e}} \left(1 - \frac{1}{\text{Pr}}\right) \frac{\partial}{\partial t} \left(U \frac{\partial U}{\partial t}\right) \quad (14)$$

The last term in equation (14) is very small and can be neglected in accordance with reference 5. The energy equation therefore is simplified to

$$U \frac{\partial H}{\partial s} + V \frac{\partial H}{\partial t} = \frac{\nu_{e,o}}{\text{Pr}} \frac{\partial^2 H}{\partial t^2} \quad (15)$$

Now it should be noted that the resulting equations (12), (13), and (15) are in the same form as the incompressible boundary-layer equations applicable to flow over a flat plate. The boundary conditions are:

when  $t = 0$

$$\left. \begin{aligned} U &= 0 \\ V &= 0 \quad \text{for } s > \hat{s} \\ V &= V_w \quad \text{for } s \leq \hat{s} \\ H &= H_w \ll 1 \end{aligned} \right\} \quad (16)$$

when  $t = \infty$

$$\dot{U} = H = 1$$

Exact affine solutions of equations (12), (13), and (15) for the transpiration-cooled regions  $s \leq \hat{s}$  are available elsewhere (e.g., ref. 8). Following the method of reference 2, the integral method is used here for the region  $s > \hat{s}$ . The Prandtl number is assumed to be unity in the solution. The momentum and energy equations and their boundary conditions are then identical. Therefore, only the solution of the momentum equation is required. Integration of equation (12) across the boundary layer yields

$$\delta_t^2 \frac{dF_1}{ds} + \frac{F_1}{2} \frac{d(\delta_t^2)}{ds} = \nu_{e,o} \left( \frac{\partial U}{\partial \eta} \right)_w \quad (17)$$



where

$$\eta = \frac{t}{\delta_t} = \frac{\int_0^y \frac{\rho}{\rho_{e,0}} dy}{\int_0^\delta \frac{\rho}{\rho_{e,0}} dy} \quad (18)$$

$$\delta_t = u_e r^\epsilon \int_0^\delta \frac{\rho}{\rho_{e,0}} dy \quad (19)$$

and the modified momentum thickness is given by

$$F_1 = \int_0^1 U(1 - U) d\eta \quad (20)$$

Before proceeding further the validity and accuracy of equation (17) which has been obtained by transforming, simplifying, and integrating the original momentum equation (2) will be discussed.

Let us consider a hypersonic boundary layer over a solid surface. A coefficient of local skin friction can be obtained here from equation (17) using a fourth degree polynomial velocity profile as

$$\frac{C_f}{2} = \frac{\tau_w}{\rho_e u_e^2} = \frac{2r^\epsilon \mu_e \sqrt{C}}{\sqrt{\frac{1260}{37} \int_0^x \rho_e \mu_e u_e r^{2\epsilon} dx}} \quad (21)$$

The more exact integrated form of the original momentum equation (2) is given in reference 4 as

$$\frac{dF_2}{dx} + F_2 \left[ (H_c + 2) \frac{1}{u_e} \frac{du_e}{dx} + \frac{1}{\rho_e} \frac{d\rho_e}{dx} + \frac{\epsilon}{r} \frac{dr}{dx} \right] = \frac{\tau_w}{\rho_e u_e^2} \quad (22)$$

where the momentum thickness is defined by

$$F_2 = \int_0^\delta \frac{\rho u}{\rho_e u_e} \left( 1 - \frac{u}{u_e} \right) dy \quad (23)$$

Equation (22) was solved in reference 4 by employing a fourth degree polynomial for the velocity profile. It can be shown that the result of the analysis of reference 4 yields exactly the same value of  $C_f/2$  as that given by equation (21) when the appropriate hypersonic approximations

of reference 5 are made. The solution, (21), gives values of  $C_f$  within 5 percent of those derived in reference 5 when  $C = 1$ . Equation (17) therefore is seen to be quite satisfactory and is a much more convenient form for the present purpose than equation (22).

Let us return to the present analysis. A seventh degree polynomial in  $\eta$  is assumed for the velocity profiles along the impervious surface ( $s > \hat{s}$ ) as

$$U = \sum_{n=1}^7 a_n \eta^n \quad (24)$$

The coefficients  $a_n$  are obtained from the boundary conditions given in (16) and from the compatibility conditions derived from equation (12). These conditions are:

when  $t = 0, \eta = 0$

$$\left. \begin{aligned} U &= V = 0 \\ \frac{\partial^2 U}{\partial t^2} &= \frac{\partial^3 U}{\partial t^3} = 0 \\ \left( \frac{\partial^2 U}{\partial s \partial t} \right) \left( \frac{\partial U}{\partial t} \right) &= v_{e,o} \left( \frac{\partial^4 U}{\partial t^4} \right) \end{aligned} \right\} \quad (25)$$

when  $t = \delta_t, \eta = 1$

$$\left. \begin{aligned} U &= 1 \\ \frac{\partial U}{\partial t} &= \frac{\partial^2 U}{\partial t^2} = \frac{\partial^3 U}{\partial t^3} = 0 \end{aligned} \right\}$$

Expressions (24) and (25) yield

$$\frac{a_1 \delta_t}{v_{e,o}} \left( \delta_t \frac{da_1}{ds} - a_1 \frac{d\delta_t}{ds} \right) = 24(35 - 20a_1) \quad (26)$$

The momentum equation (17) gives

$$\frac{v_{e,o} a_1}{\delta_t} = \frac{d}{ds} [\delta_t (0.09518 + 0.04371a_1 - 0.01832a_1^2)] \quad (27)$$

The above two equations become identical to equations (A29) and (A31), respectively, of reference 2 when  $\delta$ ,  $u_\infty$ ,  $C$ ,  $v_{\infty}$ , and  $x$  in equations (A29) and (A31) are replaced by  $\delta_t$ , 1, 1,  $v_{e,0}$ , and  $s$ , respectively.

The initial conditions for equations (26) and (27) are obtained by matching the polynomial profile at  $s = \hat{s}$  to the Blasius velocity profile which is given by the exact solutions of equations (12) and (13) for the transpiration-cooled region.

The momentum and continuity equations (12) and (13) may be transformed to the Blasius equation over a flat plate as

$$f'''' + ff''' = 0 \quad (28)$$

by letting

$$f(\eta_B) = \frac{\psi}{\sqrt{v_{e,0}s}} \quad (29)$$

$$\frac{1}{2} f'(\eta_B) = \frac{u}{u_e} \quad (30)$$

and

$$\eta_B = \frac{t}{2\sqrt{v_{e,0}s}} \quad (31)$$

The boundary conditions for equation (28) are as follows for the transpiration-cooled regions:

at  $\eta_B = 0$

$$f = f_w = -2\rho_w v_w \frac{\sqrt{\int_0^x \rho_e \mu_e u_e r^{2\epsilon} dx}}{\rho_e \mu_e u_e r^{\epsilon} \sqrt{C}} \quad (32)$$

$$f' = 0$$

at  $\eta_B = \infty$

$$f' = 2$$

The solution of equation (28) may be found in reference 8 for various values of  $f_w$ . The solution is the same as the one used for the transpiration-cooled region of reference 2 except for different definitions of independent variables.

The profiles where the transpiration-cooled region meets the solid region are approximately matched, as in reference 2, by the following method. First, the friction coefficient determined by the polynomial profile without transpiration is matched to that given by the Blasius profile with transpiration. In the present analysis, when the two expressions for  $C_f/2$  are derived and equated, there results

$$\eta_{B,\delta_t} = \frac{2a_1}{f''(0)} \quad (33)$$

Equation (33) is identical in form to equation (A49) in reference 2. Secondly, the definition of boundary-layer thickness in the Blasius solution is taken as that value of  $\eta_B$  at which

$$\frac{u}{u_e} = \frac{1}{2} f'(\eta_{B,\delta_t}) = 0.9976$$

as in reference 2. Then equation (33) yields a value of  $a_1$  at  $s = \hat{s}$  which is identical to (in the terminology of ref. 2) the value of  $a$  found for  $x = x_0$  in reference 2. It is now clear that the solution of the present equations (26) and (27) can be obtained directly from reference 2. The local skin friction over the solid surface of a blunt body downstream of the transpiration-cooled region is then given by the simple relationship, for a given  $f_w$ ,

$$\frac{C_f(s)}{C_f(s)_{f_w=0}} = \frac{\bar{C}_f(x)}{\bar{C}_f(x)_{f_w=0}} \quad (34)$$

where the ratio,  $\bar{C}_f(x)/\bar{C}_f(x)_{f_w=0}$ , is for a flat plate and is calculated in reference 2 for several values of  $f_w$ . The skin-friction ratio,  $C_f(s)/C_f(s)_{f_w=0}$ , can be transformed to the physical plane as  $C_f(x)/C_f(x)_{f_w=0}$  by use of equation (6).

The convective heat transfer for a Prandtl number of 1 may be written

$$\frac{St(s)}{St(s)_{f_w=0}} = \frac{C_f(s)}{C_f(s)_{f_w=0}} \quad (35)$$

This relationship should be valid for engineering purposes even when the Prandtl number is as low as 0.7.

## DISCUSSION

The ratios,  $C_F(x)/C_F(x)_{f_w=0}$  and  $St(x)/St(x)_{f_w=0}$ , are plotted in figure 2 for a flat plate, a circular cylinder (axis normal to flow), and a sphere for two blowing rates. In the calculations for the cylinder and the sphere, the following simple relationships were used for small  $\theta$

$$\left. \begin{aligned} u_{e,c} &= \beta_c x \\ u_{e,s} &= \beta_s x \\ \rho_e \mu_e &= (\rho_e \mu_e)_o \\ r &= x \end{aligned} \right\} \quad (36)$$

The solution for a sphere depends on the absolute value of  $\hat{\theta}$  as well as the ratio  $x/\hat{x}$ . The result for the sphere shown in figure 2 is for  $\hat{\theta} = 10^\circ$ .

The results shown in the figure are for values of the dimensionless blowing parameter  $f_w$  equal to -0.25 and -1. Equations (32) and (36) yield the following relationships between  $f_w$  and the actual blowing rate,  $\rho_w v_w$ .

For a flat plate,

$$\rho_w v_w = -\frac{1}{2} \sqrt{\frac{C_p(\rho_e \mu_e)_{p u_{e,p}}}{x}} f_w \quad (37)$$

For a cylinder,

$$\rho_w v_w = -\frac{1}{2} \sqrt{2C_c(\rho_e \mu_e)_o \beta_c} f_w \quad (38)$$

For a sphere,

$$\rho_w v_w = -\frac{1}{2} \sqrt{4C_s(\rho_e \mu_e)_o \beta_s} f_w \quad (39)$$

Consider, as a basis of comparison, the conditions for which

$$\sqrt{\frac{C_p(\rho_e \mu_e)_{p u_{e,p}}}{x}} \approx \sqrt{2C_c(\rho_e \mu_e)_o \beta_c} \approx \sqrt{4C_s(\rho_e \mu_e)_o \beta_s} \quad (40)$$

Figure 2 shows that for a given value of  $f_w$  the protection afforded to the body downstream of the transpiration-cooled region becomes less

effective when a favorable pressure gradient is imposed on the flow and when the flow is varied from two- to three-dimensional. The figure also shows that the protection from high heat-transfer rate given to the impervious surface downstream of the transpiration-cooled regions is very small near the stagnation region of a hypersonic vehicle.

It may be interesting to note that the problem of localized mass transfer cooling of rocket nozzle walls can be handled by essentially the same method as given here. This is because the density ratio,  $\rho_e/\rho_w$ , is very small along the walls of the nozzle so that the basic simplification of the hypersonic boundary layer can be made in that case also.

A  
4  
0  
9  
The present study, strictly speaking, has been concerned with localized air injection only. In the case of a localized mass transfer of a fluid other than air, however, the relative results between the three bodies (flat plate, cylinder, and sphere) should still be essentially the same as those presented here provided the transferred fluid properties do not differ greatly from those of air.

#### CONCLUDING REMARKS

The effect of localized mass transfer on skin friction and heat transfer was analyzed for the impervious surfaces downstream of the transpiration-cooled region of hypersonic blunt bodies.

Local coefficients of skin friction and Stanton numbers were calculated near the stagnation regions of a circular cylinder and a sphere for the case of localized mass transfer at the stagnation region.

The numerical results obtained here and the flat plate result of reference 2 were compared on the basis of the Blasius dimensionless fluid injection parameter. The comparisons showed that the localized mass transfer becomes less effective in protecting the downstream impervious surfaces when a favorable pressure gradient is imposed on the flow and when the flow is varied from two- to three-dimensional.

Ames Research Center  
National Aeronautics and Space Administration  
Moffett Field, Calif., Feb. 19, 1960

## REFERENCES

1. Howe, John T.: Some Finite Difference Solutions of the Laminar Compressible Boundary Layer Showing the Effects of Upstream Transpiration Cooling. NASA MEMO 2-26-59A, 1959.
2. Rubesin, Morris W., and Inouye, Mamoru: A Theoretical Study of the Effect of Upstream Transpiration Cooling on the Heat-Transfer and Skin-Friction Characteristics of a Compressible, Laminar Boundary Layer. NACA TN 3969, 1957.
3. Libby, Paul A., and Pallone, Adrian: A Method for Analyzing the Heat Insulating Properties of the Laminar Compressible Boundary Layer. Jour. Aero. Sci., vol. 21, no. 12, Dec. 1954, pp. 825-834. A  
4  
0  
9
4. Libby, Paul A.: The Laminar Hypersonic Heat Transfer on a Blunt Body According to the Integral Method. Heat Transfer and Fluid Mechanics Institute, Preprints of papers, 1958, pp. 216-230.
5. Lees, L.: Laminar Heat Transfer Over Blunt-Nosed Bodies at Hypersonic Flight Speeds. Jet Propulsion, vol. 26, no. 4, April 1956, pp. 259-269.
6. Lees, L.: Convective Heat Transfer With Mass Addition and Chemical Reactions. Combustion and Propulsion, Third AGARD Colloquium, Palermo, Sicily, March 17-21, 1958, Pergamon Press, N.Y., pp. 451-498. (Also Calif. Inst. of Tech., Guggenheim Aero. Lab., Pub. 451.)
7. Kemp, Nelson H., Rose, Peter H., and Detra, Ralph W.: Laminar Heat Transfer Around Blunt Bodies in Dissociated Air. Jour. Aero./Space Sci., vol. 26, no. 7, July 1959, pp. 421-430. (Also AVCO Res. Lab. Rep. 15, 1958.)
8. Low, George M.: The Compressible Laminar Boundary Layer With Fluid Injection. NACA TN 3404, 1955.

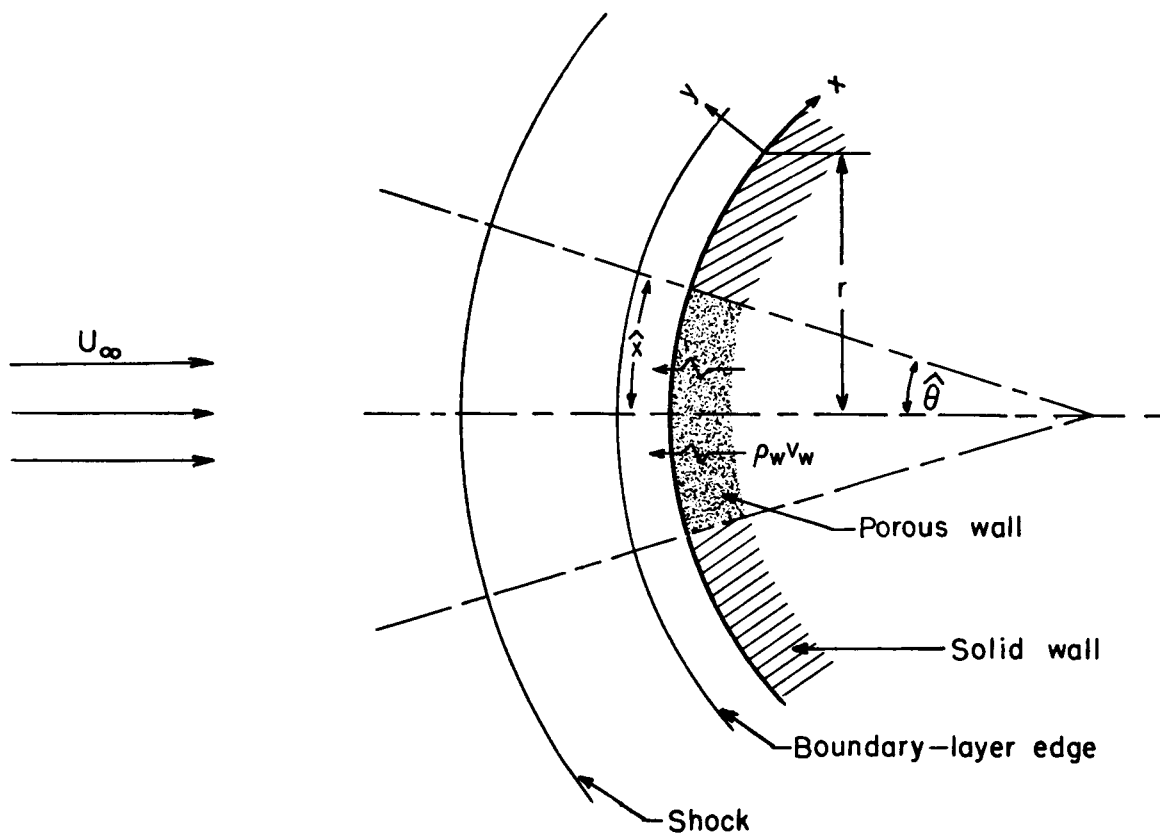


Figure 1.- Physical model used in the sample calculation.



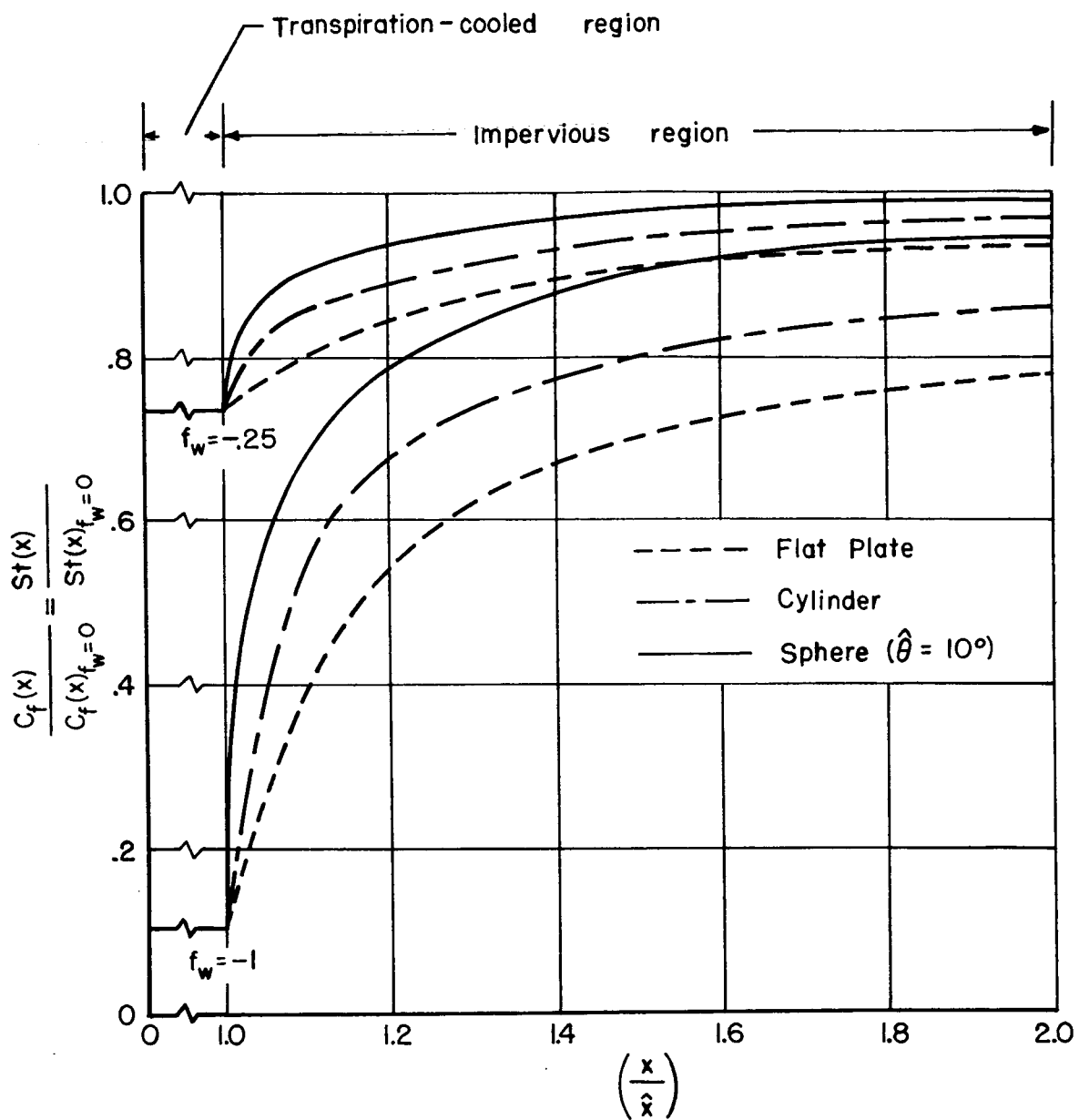


Figure 2.- Effect of localized mass transfer.